Author's Accepted Manuscript

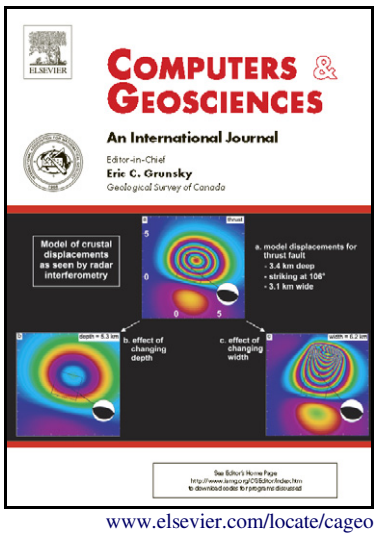

www.elsevier.com/locate/cageo

MARD-A Moving Average Rose Diagram application for the Geosciences

Mark A. Munro, Thomas G. Blenkinsop

PII: S0098-3004(12)00251-8
DOI: http://dx.doi.org/10.1016/j.cageo.2012.07.012
Reference: CAGEO2967

To appear in: *Computers & Geosciences*

Received date: 29 March 2012
Revised date: 2 July 2012
Accepted date: 3 July 2012

Cite this article as: Mark A. Munro and Thomas G. Blenkinsop, MARD-A Moving Average Rose Diagram application for the Geosciences, *Computers & Geosciences,* http://dx.doi.org/10.1016/j.cageo.2012.07.012

MARD – A **M**oving **A**verage **R**ose **D**iagram application for the Geosciences

Mark A. Munro*, Thomas G. Blenkinsop

School of Earth & Environmental Sciences, James Cook University, Townsville, Queensland 4811, Australia. Telephone: (+61) 7 4781 6909. Email: mark.munro@my.jcu.edu.au

Abstract

MARD 1.0 is a computer program for generating smoothed rose diagrams by using a moving average, which is designed for use across the wide range of disciplines encompassed within the Earth Sciences. Available in MATLAB®, Microsoft® Excel and GNU Octave formats, the program is fully compatible with both Microsoft® Windows and Macintosh operating systems. Each version has been implemented in a user-friendly way that requires no prior experience in programming with the software. MARD conducts a moving average smoothing, a form of signal processing low-pass filter, upon the raw circular data according to a set of pre-defined conditions selected by the user. This form of signal processing filter smoothes the angular dataset, emphasising significant circular trends whilst reducing background noise. Customisable parameters include whether the data is uni- or bi-directional, the angular range (or aperture) over which the data is averaged, and whether an unweighted or weighted moving average is to be applied. In addition to the uni- and bi-directional

options, the MATLAB® and Octave versions also possess a function for plotting 2-dimensional dips/pitches in a single, lower, hemisphere. The rose diagrams from each version are exportable as one of a selection of common graphical formats. Frequently employed statistical measures that determine the vector mean, mean resultant (or length), circular standard deviation and circular variance are also included. MARD's scope is demonstrated via its application to a variety of datasets within the Earth Sciences.

Keywords: Rose Diagram, Moving average, Circular statistics, Vector mean, MATLAB®, Microsoft® Excel

1. Introduction

Moving averages, sometimes referred to as running averages, are a form of signal processing filter which produce averages of subsets of data series from within the master data series in 1-dimension. Data filtering of this kind serves a broad variety of applications within science and engineering, being primarily utilised to accentuate trends in data that are otherwise generally less apparent, or to recover meaningful signal components by removing the high-frequency noise. Other uses include 2-dimensional enhancements in the resolution of graphics, and providing a form of interpolation that generates intermediate values. Within the Earth Sciences, such analyses are commonly applied in various forms for image processing of aerial photographs, maps and satellite images (Diniz da Costa & Starkey, 2001; Jordan, 2007). Moving averages may be applied to rose diagrams that depict azimuthal data.

At present, moving average rose diagrams are not commonly used within the Earth and Environmental Sciences; however, they are a very effective means of visualisation (e.g. Aerden, 2003; 2004; Aerden & Sayab, 2008). The most obvious benefit of this representation is that the commonly segmented, or 'blocky' appearance of rose plots, due to aggregation of data in bins, is avoided.

A range of good quality software is available for plotting geoscience data on both Mac and Windows platforms. Within these programs, rose diagrams are a common function. Examples include *GEOrient*© (Holcombe, 1994), *Spheristat*™, *RJS graph, Stereonet*©, *OSXStereonet*©, *Grapher*™, *KaleidaGraph*©, *Rose.C* (Kutty & Ghosh, 1992) and *EZ-Rose* (Baas, 2000). However, only one of these, *Spheristat*™, presents a 'smoothing' function for rose and polar diagrams that is similar to a moving average filter. This program is relatively expensive to purchase and is only available for Windows.

The primary aim of this paper is to promote the use and benefits of moving average filters within rose diagrams via the provision of freely distributable, user-friendly programs which do not require any prior knowledge of high-level programming languages. Three formats are presented for users to readily produce a moving average rose diagrams on either Windows or Macintosh platforms. MARD is available 1) as a script written for MATLAB®, 2) a script for GNU Octave and 3), a macro implemented for use in conjunction with Microsoft Excel. The benefits of MARD are illustrated via its application to a diverse range of datasets within the Earth and Environmental sciences.

2. Moving average rose diagrams: overview and evaluation

76

77 *2.1. Moving average rose diagrams: a definition*

78

79 When presenting rose diagrams, the most common convention within the
80 Earth Sciences is to represent azimuthal data utilising 10° bins, the frequencies of
81 which represent the sum of all of the azimuths within that bin. Binning is used in
82 order to emphasise major trends in data, but inherently loses a certain level of detail
83 because the distribution of data within the bins is unknown. Moreover, the arbitrary
84 selection of bin width and boundaries may have a significant impact upon the result.
85 Moving average rose diagrams, on the other hand, evaluate the frequency of
86 each azimuth within the context of those in immediate proximity to it. The frequency
87 of each azimuth, and those of azimuths within a pre-defined range (the aperture, or
88 moving window) either side of it are systematically summed and averaged. The
89 resultant average for each azimuth is then assigned to the central value position and
90 plotted on the final rose diagram. The broader the aperture, the greater the smoothing
91 effect.

92

93 *2.2. Types of moving average: weighted versus unweighted*

94

95 Moving averages may be either unweighted (a.k.a. a 'simple' moving average)
96 or weighted. Where no weighting is applied, each azimuth frequency within the
97 aperture is counted as its full value, i.e. each is deemed equally important in
98 determining the local average:

99

100
$$M_\alpha = \frac{1}{A} \sum_{i=\alpha-\frac{A-1}{2}}^{n=\alpha+\frac{A-1}{2}} F_i \qquad (1)$$

101 where: M_α is the unweighted average value to be subsequently plotted on the rose

102 diagram for that azimuth, α is the azimuth for which the average is determined, F_i is

103 the raw frequency at angle i, A is the aperture size.

104 Alternatively, when a weighted moving average is applied, the raw values of
105 the data in azimuths outside the central one are reduced by a magnitude that depends
106 upon their proximity to the centre. The raw value of immediately adjacent data is
107 reduced by less than those nearer to the margins of the aperture. Weighting permits
108 more emphasis to be placed upon those data closer to the centre of the aperture. A
109 weighted mean is thus less than, and represents a proportion of, an equivalent
110 unweighted mean.

111 In many applications, especially when dealing with large datasets, unweighted
112 moving averages are appropriate. However, in a number of circumstances the
113 application of a weighted average might be more beneficial. One such example is
114 when handling small datasets. In particular, where data is clustered, an unweighted
115 moving average may result in a 'plateau' distribution like a binned plot. The use of a
116 weighted moving average in scenarios such as this provides a means of smoothing the
117 data markedly whilst still preserving the local maxima.

118

119 *2.3. Weighted moving averages in MARD*

120

In MARD, weight is distributed among the azimuths in a non-linear fashion, because linear methods are intrinsically restrictive: for example, reducing each value progressively by 10% from the central position can only be achieved for 10 positions either side before becoming negative. However, the non-linear method is applicable to any aperture. The user specifies a proportion, expressed as the weighting factor, which reduces the contribution of each neighbouring raw value with increasing distance from the reference position. Thus, in calculating the moving average around an azimuth of 87° using a weighting factor of 0.9, the frequencies of data at azimuths of 86° and 88° (one position removed from the centre) are reduced to 0.9 of their full values, and the frequencies at azimuths of 85 and 89° (two positions removed) are reduced to a proportion of 0.9 x 0.9 = 0.81 of their full values. The moving average for that azimuth is then the average of these weighted values within the aperture in the same manner as an unweighted average, and is represented as:

$$Mw_{\alpha} = \frac{1}{A} \sum_{i=\alpha-\frac{A-1}{2}}^{n=\alpha+\frac{A-1}{2}} F_i \cdot w^{\left|\alpha-\frac{A-1}{2}\right|} \qquad (2)$$

where: Mw_{α} is the weighted average value to be subsequently plotted on the rose diagram for that azimuth, α is the azimuth for which the average is determined, F_i is the raw frequency at angle i, A is the aperture size, w is the value of weighting factor applied.

2.4. The 'up-scaling factor' for weighted moving averages

One effect of weighting the averages as described above is that it lowers the frequencies of the plot relative to those within an equivalent unweighted plot. The degree to which this occurs is proportional to the degree of weighting applied. Where the adjacent values are still weighted relatively strongly (e.g. a weighting factor of 0.95) then the frequencies will not be reduced to a large degree. On the other hand, if the adjacent values are allocated much lower weight than the central (e.g. 0.7) then the magnitude of frequencies will be reduced considerably more, resulting in a notable loss in magnitude of the moving average.

In order to counter-act this effect, an 'up-scaling factor' is applied to the weighted moving average frequencies. The value of this factor is inversely proportional to the value of weighting factor selected and is given as:

$$\frac{1}{D} = 1 + 2\sum_{i=1}^{n=\frac{A-1}{2}} w^i \qquad (3)$$

where: $1/D$ is the up-scaling factor, A is the aperture size, w is the weighting factor. To upscale the weighted moving average, the proportion of the equivalent unweighted mean that the value of the weighted mean should represent is calculated for the selected aperture size and weighting factor applied. Each weighted frequency is then multiplied (up-scaled) by the inverse of this proportion. This restores the absolute frequencies back into a range equivalent to that of an unweighted moving average, so that they can be compared to the unweighted moving averages.

2.5. Benefits and Limitations

The primary advantage of moving average rose diagrams over their binned counterparts is the removal of the coarse, blocky appearance of the former, with artificial steps at bin boundaries. The product is a plot that is more visually appealing and notably more informative. Moreover, the suppression of minor variations by averaging accentuates significant changes or trends in the data. The main objective of applying moving averages to a dataset is to smooth the plot to emphasise the significant trends present, whilst retaining its original character as much as possible. Filtering data in this way inherently provides more context for the distribution of frequencies around the compass, and within individual bins, than conventional plots. Consequently, moving averages commonly reveal a more accurate representation of the distribution of modal maxima within a dataset than are otherwise portrayed in an equivalent binned counterpart (Fig. 1).

One limitation of the moving average method by calculating a mean value (as implemented in MARD) is that it may potentially be influenced by outliers, i.e. spurious maxima. A median average method (e.g. Jordan, 2007) may ameliorate this problem, and this could be implemented in future versions of MARD. At present, however, the mean method is proposed because it is the most common and readily understood type of moving average.

[FIGURE 1]

3. Implementing moving average rose diagrams: adjustable parameters

In the MARD program the user pre-defines a number of parameters; data type (this determines how the data are handled), number of datasets to be plotted,

unweighted or weighted averaging, the magnitude of weighting (if applicable), and the sampling aperture (angular window over which the data is to be averaged). The following section addresses the principal considerations associated with each of the above.

3.1. Data type

MARD handles three types of data. "Uni-directional" is implemented for use with uni-directional data, i.e. vectors that have a unique direction and therefore one compass azimuth only, for example palaeocurrents. "Bi-directional", is designed for use with bi-directional data, i.e. lines that are specified by one azimuth as well as the complementary one at 180°, for example the strikes of planar features such as bedding or tectonic foliations. The distinction between uni- and bi-directional data is sometimes referred to as the difference between directional and oriented data (Davis 2002). The third data type (MATLAB® and Octave versions only) was incorporated primarily for representing porphyroblast inclusion trail pitches, a common application in microstructural geology. For this data type, MARD generates a single semicircle below a diameter that represents an artificial horizontal reference. Data represent the inclination, or pitch, of each element from the horizontal reference plane, with those inclined to the right of the page trending towards a given compass orientation and those to the left towards its complement.

A selection of circular statistical functions commonly utilised to evaluate such datasets are also included. These include the vector mean, mean resultant, circular standard deviation and circular variance/dispersion (Fisher, 1993; Davis, 2002; Pewsey, 2004; Allmendinger et al, 2012). These functions are equipped to handle

both integer and non-integer values. A number of fully comprehensive circular statistics toolboxes are already available for MATLAB® (Jones, 2006; Berens & Velasco, 2009). The vector statistics capability of MARD is not intended as a replacement for these, but is incorporated for convenience.

3.2. Number of datasets to be plotted

The operator specifies the number of datasets they wish to be plotted in the rose diagram (MATLAB® and Octave versions only). Each dataset is then input independently when prompted. Generally it is recommended that no more than three datasets be plotted at once to avoid overpopulating the rose.

3.3. Aperture

Apertures are designated by odd values, so that the resultant average is positioned in the central location within it. The aperture size exerts first-order control upon the appearance of the resultant moving average plot. The lower the aperture, the closer the plot will resemble the raw, unaveraged, data, plotted in 1° increments. This assumes that the data being dealt with are in integer degree format, however directional data may also be non-integer. If the latter are input, they are automatically rounded to the nearest integer prior to counting. As the aperture is increased, the plot becomes progressively more generalised, i.e. smoother (Fig. 2). The more irregular the original dataset is, the larger the aperture that may be required in order to smooth it. Consequently, the user's discretion is necessary to decide which aperture is most suitable for any given plot. One convention is to start with the unaveraged plot (1°)

and incrementally increase the aperture by 2° until the desired effect is achieved. However, in our experience we have found an aperture of 9° to prove a suitable benchmark. For some datasets an aperture of as little as 5° may be sufficient, however others may require a significantly greater value. Some previously published moving average roses (e.g. Aerden, 2003; 2004; Aerden & Sayab, 2008) have utilised apertures of 21°, which have produced appropriate smoothing.

[FIGURE 2]

It is also important to preserve the essence of the data such that it is still representative of the original and does not become biased or highly distorted. Beyond a certain value of aperture the data will begin to homogenise as apertures are progressively increased, amalgamating the major trends and becoming too generalised (e.g. Fig. 2d). This arises due to the large portions of the data now being averaged, with each aperture averaging essentially the same sub-set. Thus, the aperture utilised is dependent upon what the user wishes to highlight and to what degree they wish to preserve the minor peaks.

3.4. Selecting an appropriate weighting factor

The largest weighting factor of 1 will return the same values as an unweighted average, whereas a minimum possible factor of 0 will produce a scaled-down version of the original non-averaged dataset. Thus, there is an inherent limit to the value of weighting factor that may be applied to smooth a particular dataset before it begins to resemble the original dataset. For this reason, we recommend using weighting factors

between 1.0 and 0.7. These values are sufficient to smooth the data, whilst remaining sufficiently different to the original dataset. It is advisable to begin with a higher weighting factor (e.g. 0.95) and progressively decrease the value in 0.05 increments until the smoothing is sufficient. Values of 0.95 or 0.9 are most commonly adequate. The effects of applying different weighting factors are illustrated in figure 3.

[FIGURE 3]

3.5. Equal area option

Commonly used rose diagrams with a linear radial scale for frequency generate visual bias due to the widening of a petal as it extends outwards from the origin (Nemec, 1988). Frequencies may appear notably more or less prominent relative to those surrounding them in a manner disproportionate to their absolute differences in magnitude, potentially promoting mis-interpretations of apparent preferred orientations (Nemec, 1988; Wells, 1999; 2000; Baas, 2000; Davis, 2002; Borradaile, 2003). This bias is avoided in an equal-area rose diagram, in which the sector area, as opposed to the length, is proportional to the frequency. MARD therefore also offers the option of accounting for this bias via plotting the square root of each of the original moving average frequencies (cf. Davis, 2002; Borradaile, 2003). We recommend that this should be the default type of rose diagram. Figure 4 conveys the impact of employing equal area roses compared to an equivalent linearly-scaled plot; the former producing a more representative depiction of the relative strength of frequencies.

[FIGURE 4]

4. Using MARD

The three versions of MARD are each operated slightly differently and utilise separate software packages, offering users maximum flexibility and preference. A quick reference comparison guide is found in Table 1.

[TABLE 1 HERE]

4.1. The MATLAB® version

The MATLAB® script has been designed to be used straightforwardly and efficiently by even those with no prior knowledge of programming with the software. Data is input in the same manner for both the uni- and bi-directional types, as single absolute compass azimuths. This may be done manually or via pasting directly from a text editor. However, for bi-directional data, each azimuth is automatically replicated as its complement. A direction pertaining to azimuths of 000° and 180° may be entered as either value. Pitch/plunge data are handled differently. As each value represents a pitch from the horizontal, data are entered as pitch values between 0° and 90°, with those inclined to the right with respect to the plot as positive and those inclined to the left as negative. Alternatively, if preferred, pitches may be entered as their equivalent absolute compass values between 90° and 270°.

To produce the visual rose diagram output, MATLAB®'s in-built function for polar plots (*polar.m*) is called. This function plots each moving average value or

315 increment versus its associated azimuth in radians. Once output, MATLAB® permits
316 modifications of the plot to a degree via its built-in *property editor*, which permits
317 saving the plot in a range of commonly utilised graphics formats. However, we
318 recommend exporting diagrams in *.eps* format instead, allowing for more
319 comprehensive customisation of every element of the rose diagram in any vector-
320 based illustration package such as Adobe® Illustrator®, CorelDraw®, Canvas™,
321 OpenOffice or Freehand® (Fig. 5). The contents of each independent array can be
322 accessed once the graphical output has been produced.
323
324 [FIGURE 5]
325
326 *4.2. The GNU Octave version*
327
328 Octave has been developed as a freeware equivalent to MATLAB®, presenting
329 almost direct compatibility for *.m* files utilised and produced by the former (Eaton et
330 al., 2008). A freely distributed manual for the software is available online, or a print
331 version may be purchased for a modest fee. Octave utilises the system's command
332 terminal shell and calls upon an independent graphics terminal to produce visual plots,
333 which may be Aquaterm, or x11 (Macintosh) or Cygwin, or Gnuplot (Windows). The
334 Octave version of MARD is almost identical to the MATLAB® version and presents a
335 highly similar user interface. Therefore, the operating instructions for this version are
336 as above. However, Octave's polar plot format is initially somewhat different, and
337 requires some quick-fix modifications to the output (Fig. 6). The circular statistics
338 capability of the Octave version of MARD is also identical to that of the MATLAB®
339 version.

[FIGURE 6]

4.3. The Microsoft® Excel version

Since Microsoft® Excel is compatible with Visual Basic for Applications in both the latest Windows and Mac versions, it was logical to use VBA code to generate the output for plotting with the radar function. This is contained in the "Rose" macro subroutine contained in Module1 of the Excel workbook. The Microsoft Excel version of MARD utilises the standard "radar plot" in Excel, which is a crude type of rose diagram. Data are entered into column A of the Excel MARD spreadsheet, starting at row 4. Row 1 contains a number of drop-down menus to set the adjustable parameters, including whether the data is Uni or Bidirectional, the Aperture ($1 \leq$ Aperture ≤ 35) and the weighting factor ($1 \geq w \geq 0.5$, in 0.05 increments). The program is run from the "Tools" menu by selecting the "Rose" macro. This version of MARD does not possess the lower hemisphere option offered in MATLAB® and Octave, nor the capacity for plotting multiple data sets.

The averaged data for plotting in the rose diagram are output in column H, commencing at row 4. These are scaled and plotted automatically. A range of features such as the plot title, font sizes and colour(s) may be readily formatted in the usual way in Excel. Unlike the previous two versions, outputs from Excel (e.g. Fig. 7) cannot be exported in vector-based graphics formats.

[FIGURE 7]

5. Applications

5.1. "Uni-directional" option (all versions)

The "uni-directional" option is demonstrated via its application to palaeocurrent orientations, a valuable tool in sedimentology and stratigraphy. Field measurements of the foresets of trough cross-bedding, a structure developed during uni-directional flow in fluvial, marine and aeolian systems, are frequently employed in the reconstruction of flow regimes and sedimentary provenance. Figs. 1(a) and 3 depict palaeocurrent trends extracted from sandstones at Porcupine gorge, Queensland, Australia (Roberts et al., unpubl. data) and the mid-Cretaceous Dinosaur Beds of Malawi, Africa (Roberts et al., 2010: Fig. 16) respectively. Microfracture orientations (Fig. 8) extracted from 25 Garnet porphyroclasts within the Mtilikwe shear zone, Zimbabwe, which have been interpreted as shear sense indicators (Blenkinsop & Kisters, 2005) are also presented.

Further applications for this option include the orientations of glacial striations (Davis, 2002), the trends of intersection, crenulation or mineral elongation lineations, and fold hinges. The lineations and fold hinges (common measurements in structural geology) are unidirectional because of the convention that their azimuths are recorded down plunge. Vertebrate bone orientations in sedimentary units have long been employed as a form of palaeocurrent indicator (e.g. Voorhies, 1969; Behrensmeyer, 1982; 1987; Tucker, 2011). Vertebrate bone orientations in which one condyle is larger than the other can be utilised to constrain flow direction to a single azimuth. Bones with substantial aspect ratios and a well-defined long axis such as the femur, radius and humerus (Voorhies, 1969) assume spatial orientations indicative of flow

direction at the time of deposition. The long axes of coalified logs have also been used as palaeocurrent indicators in a similar manner (Eberth & Currie, 2010) and also to infer ash flow direction (Roberts & Hendrix, 2000).

[FIGURE 8]

5.2. "Bi-directional" option (all versions)

Figs. 1(b) and 4(b) represent the strikes of porphyroblast inclusion trails from the classic High-Temperature Low-Pressure Cooma Metamorphic Complex of S. E. Australia. The inclusion trail strikes are those of sub-vertical internal foliations preserved within Andalusite and K-feldspar, measured via mechanical stage from horizontal thin sections. Such measurements are extremely useful in evaluating whether the porphyroblasts have been subject to significant rotation during subsequent deformation events.

Figs. 5, 6 and 7 depict long axis orientations of *Syntarsis rhodesiensis* (Dinosauria, theropoda) bones within a sedimentary sequence from Zimbabwe (Roberts et al, unpubl. data). These are considered bi-directional as opposed to the aforementioned uni-directional sets utilised for palaeocurrents because they are not associated with one specific azimuth (i.e. flow direction) and thus are represented as both.

Additional applications of this function include the long axes orientations of igneous phenocrysts or granite bodies, (e.g. Blenkinsop & Treloar, 2001), dyke trends (Klausen, 2006), fault strikes (Wechsler et al., 2010), shear zone strikes (Blenkinsop

et al., 1990) and the axial traces of folds. The latter are distinguished from fold hinges, which are uni-directional measurements.

5.3. "Pitches/plunges" option (MATLAB® & Octave versions only)

The "pitches/plunges" option is illustrated via the plotting of 2-Dimensional porphyroblast internal inclusion trail pitches from the classic Cooma Metamorphic Complex of S. E. Australia. The inclination of internal foliation pitches from the horizontal were measured directly from microscope thin sections using a mechanical stage. The inclusion trails were measured perpendicular to their strikes, in order to obtain their true pitches. This was conducted for andalusite and cordierite porphyroblasts (Fig. 9), both of which proved insightful in reconstructing the tectono-metamorphic history of the complex. The consistency of inclusion trail pitches exhibited by the rose diagrams, in conjunction with other microstructural and mesoscale evidence, is highly suggestive that the inclusion trails are representative of their initial orientations. Such pitch measurements have been made in several publications on inclusion trails (e.g. Hayward, 1992; Johnson, 1992; Aerden, 1995), however the moving average rose diagrams presented here have a more informative appearance than the commonly utilised format of 10° binned data.

[FIGURE 9]

6. Conclusions

Moving averages are an under-utilised form of analysis when dealing with circular, or vector, data in the Earth Sciences, perhaps because of the lack of moving average functionality in almost all available software used to produce rose diagrams. The dearth of moving average rose diagrams may be further enhanced by a lack of awareness of the benefits and potential use of moving averages when dealing with orientation data. To this end, MARD is presented in several formats such that it is readily available to the scientific community, and has been designed for ease-of-use. The examples of moving average rose diagrams above illustrates their broad applicability to numerous and diverse fields in Earth Sciences. They serve to reduce the background noise of the plots, and render significant trends readily apparent. When incorporating moving average rose diagrams in publications it is important to specify the number of elements within sample analysed, the aperture, whether linear scaling or equal area representations are used, and any weighting factor utilised in the on the figure or in the figure caption. Moreover, when plotting multiple rose diagrams for comparison with one another in the same figure, we recommend utilising the same set of parameters in each.

Acknowledgements

We wish to thank E. M. Roberts and R. T. Tucker for insightful discussions regarding the representation of data and their willing provision of cross-bedding trends and dinosaur bone orientations for demonstration of the program. P. J. Higgins is also thanked for sharing his extensive experience and raising constructive suggestions

which provided some more elegant solutions to operations in the MATLAB® and Octave scripts. The two journal referees made useful criticisms.

References

Aerden, D.G.A.M., 1995. Porphyroblast non-rotation during crustal extension in the Variscan Lys-Caillaouas Massif, Pyrenees. Journal of Structural Geology 17, 709-725.

Aerden, D.G.A.M., 2003. Preferred orientation of planar microstructures determined via statistical best-fit of measured intersection-lines: the 'FitPitch' computer program. Journal of Structural Geology 25, 923-934.

Aerden, D.G.A.M., 2004. Correlating deformation in Variscan NW-Iberia using porphyroblasts; implications for the Ibero-Armorican Arc. Journal of Structural Geology 26, 177-196.

Aerden, D.G.A.M., Sayab, M., 2008. From Adria- to Africa-driven orogenesis: Evidence from porphyroblasts in the Betic Cordillera, Spain. Journal of Structural Geology 30, 1272–1287.

Allmendinger, R.W., Cardozo, N., Fisher, D.M., 2012. Structural Geology Algorithms, 1st Edn., Cambridge University Press, Cambridge, 289pp.

Baas, J.H., 2000. EZ-ROSE: a computer program for equal-area circular histograms and statistical analysis of two-dimensional vectorial data. Computers & Geosciences 26, 153-166.

Behrensmeyer, A.K., 1982. Time resolution in fluvial vertebrate assemblages. Paleobiology 8, 211-227.

Behrensmeyer, A.K., 1987. Vertebrate preservation in fluvial channels. Palaeogeography, Palaeoclimatology, Palaeoecology 63, 183-199.

Berens, P., Velasco, M.J., 2009. CircStat: A MATLAB Toolbox for Circular Statistics. Journal of Statistical Software 31, issue 10.

Blenkinsop, T. G., Dhilwayo, and Muranda, S.C. 1990. Intracratonic shearing on shear zones of the Mushandike granite, Zimbabwe. Proceedings of the Second Symposium of Science and Technology, Research Council of Zimbabwe, IIA, 396-421.

Blenkinsop, T.G., Kisters, A.F.M. 2005. Steep extrusion of late Archean granulites in the Northern Marginal Zone, Zimbabwe; evidence for secular change in orogenic style. Geological Society of London Special Publications 243, 193-204, doi:10.1144/GSL.SP.2005.243.01.14

Blenkinsop, T.G., Treloar, P.J., 2001. Tabular intrusion and folding of the late Archaean Murehwa granite, Zimbabwe, during regional shortening. Journal of the Geological Society of London 158, 653-664.

512

513 Borradaile, G.J., 2003. Statistics of Earth Science data: their distribution in time,

514 space and orientation, 1st Edn., Springer, 351pp.

515

516 Davis, J.C., 2002. Statistics and Data Analysis in Geology, 3rd Edn., John Wiley &

517 Sons, 656pp.

518

519 Diniz da Costa, R., Starkey, J., 2001. PhotoLin: a program to identify and analyze

520 linear structures in aerial photographs, satellite images and maps. Computers &

521 Geosciences 27, 527-534.

522

523 Eaton, J.W., Bateman, D., Hauberg, S., 2008. GNU Octave Manual Version 3,

524 Network Theory Limited, 568pp.

525

526 Eberth, D.A., Currie, P.J., 2010. Stratigraphy, sedimentology, and taphonomy of the

527 *Albertosaurus* Bonebed (upper Horseshoe Canyon Formation; Maastrichtian),

528 southern Alberta, Canada. Canadian Journal of Earth Sciences 47, 1119-1143.

529

530 Fisher, N.I., 1993. Statistical Analysis of Circular Data, 1st Edn., Cambridge

531 University Press, New York, NY, 277pp.

532

533 Hayward, N., 1992. Microstructural analysis of the classical spiral garnet

534 porphyroblasts of south-east Vermont: evidence for non-rotation. Journal of

535 Metamorphic Geology 10, 567-587.

536

Holcombe, R.J., 1994. GEOrient - an integrated structural plotting package for MS-Windows. Geological Society of Australia Abstracts 36, 73-74.

Johnson, S.E., 1992. Sequential porphyroblast growth during progressive deformation and low-P high-T LPHT) metamorphism, Cooma Complex, Australia: the use of micro- structural analysis to better understand deformation and metamorphic histories. Tectonophysics 214, 311-339.

Jones, T.A., 2006. MATLAB functions to analyze directional (azimuthal) data—I: Single-sample inference. Computers & Geosciences 32, 166-175.

Jordan, G., 2007. Adaptive smoothing of valleys in DEMs using TIN interpolation from ridgeline elevations: An application to morphotectonic aspect analysis. Computers & Geosciences 33, 573-585.

Klausen, M.B., 2006. Geometry and mode of emplacement of dike swarms around the Birnudalstindur igneous centre, SE Iceland. Journal of Volcanology and Geothermal Research 151, 340-356.

Kutty, T.S., Ghosh, P., 1992. Rose.C: a program in `C' for producing high-quality rose diagrams. Computers & Geosciences 18, 1195-1211.

Nemec, W., 1988. The shape of the rose. Sedimentary Geology 59, 149-152.

Pewsey, A., 2004. The Large-Sample Joint Distribution of Key Circular Statistics.

562 Metrika 60, 25-32.

563

564 Roberts, E.M., Hendrix, M.S., 2000. Taphonomy of a Petrified Forest in the
565 Two Medicine Formation (Campanian), Northwest Montana: Implications for
566 Palinspastic Restoration of the Boulder Batholith and Elkhorn Mountain Volcanics.
567 Palaios 15, 476–482.

568

569 Roberts, E.M., O'Connor, P.M., Stevens, N.J., Gottfried, M.D., Jinnah, Z.A., Ngasala,
570 S., Choh, A.M., Armstrong, R.A., 2010. Sedimentology and depositional
571 environments of the Red Sandstone Group, Rukwa Rift Basin, southwestern
572 Tanzania: New insight into Cretaceous and Paleogene terrestrial ecosystems and
573 tectonics in sub-equatorial Africa. Journal of African Earth Sciences 57, 179-212.

574

575 Tucker, R.T., 2011. Taphonomy of Sheridan College Quarry 1, Buffalo, Wyoming:
576 Implications for reconstructing historic dinosaur localities including Utterback's
577 1902–1910 Morrison dinosaur expeditions. Geobios 44, 527–541.

578

579 Voorhies, M.R., 1969. Taphonomy and population dynamics of an early Pliocene
580 Vertebrate Fauna, Knox County, Nebraska. Contributions to Geology Special Paper
581 No. 1, University of Wyoming, 69p.

582

583 Wechsler, N., Ben-Zion, Y., Christofferson, S., 2010. Evolving geometrical
584 heterogeneities of fault trace data. Geophysical Journal International 182, 551–567.

585

586 Wells, N.A., 1999. ASTRA.BAS: a program in QuickBasic 4.5 for exploring rose

587 diagrams, circular histograms and some alternatives. Computers & Geosciences 25,
588 641-654.

589

590 Wells, N.A., 2000. Are there better alternatives to standard rose diagrams? Journal
591 of Sedimentary Research 70, 37-46.

592

593

594 **Figure & Table Captions:**

595

596 **Table 1.** Comparison of the main features of MARD between each of the three
597 versions.

598

599 **Figure 1.** Comparisons of conventional 10° binned rose plots (the left side) versus the
600 same datasets plotted as moving averages (the right side). The binned plots were
601 produced in GEOrient (Holcombe, 1994). **a)** Palaeocurrent trends from Porcupine
602 Gorge, Queensland, Australia. n = 81, aperture = 11°, weighting factor = 0.9. **b)**
603 Strikes of inclusion trails in K-feldspar measured from horizontal thin sections
604 extracted from the Cooma Metamorphic Complex, NSW, Australia. n = 765, aperture
605 = 9°, weighting factor = 0.9. Note that the azimuthal locations of modal maxima are
606 masked in the binned plots, but evident in their moving average counterparts. All
607 plots equal area.

608

609 **Figure 2.** Series of moving average roses depicting the effect of progressively
610 increasing the value of analysis aperture for the same dataset. The data are inclusion
611 trail pitches in andalusite porphyroblasts from the Cooma Metamorphic Complex, S.E.

Australia. **a)** The original, non-averaged, data (i.e. 1° aperture). **b-d)** Apertures of 5°, 9° and 13° respectively. Note that the data becomes progressively smoother with increasing aperture. However, observe in **(d)** that the aperture size of 13° has over-generalised the plot. Thus, 9° is the best selection in this scenario; it smoothes the data sufficiently but preserves the important features. n = 1446. All plots unweighted and equal area.

Figure 3. Series of rose diagrams conveying the effect of altering the value of weighting factor applied to a moving average for the same dataset at a constant aperture of 15°. **a)** An unweighted moving average, or weighting factor of 1.0. **b-d)** Progressively decreasing values of 0.95, 0.9 and 0.85 respectively. Note that the plot becomes notably smoother and less 'blocky' than the unweighted equivalent. The data are palaeocurrent trends measured from the sandstones of the Dinosaur Beds of Malawi (Roberts et al., 2010). n = 62. All plots equal area.

Figure 4. Comparisons of equal area plots (the right side) versus their equivalent linearly scaled plots (the left side) for constant apertures and weighting factors. **a)** Palaeocurrent trends extracted from Porcupine Gorge, Queensland, Australia. n = 81, aperture = 11°, weighting factor = 0.9. Note that the notably stronger central peak in the frequency-proportional plot is evidently less important relative to the others when plotted as equal area. **b)** Strikes of inclusion trails in andalusite measured via horizontal thin sections from the Cooma Metamorphic Complex, NSW, Australia. n = 458, aperture = 9°, weighting factor = 0.9. The equal area plot reveals that the inclusion trail strikes have a greater range than is otherwise evident in the frequency-

636 proportional plot; hence the apparent widening. This is a common, inadvertent, mis-
637 representation in inclusion trail studies of this kind.
638
639 **Figure 5. a)** An unmodified output from the MATLAB® version of MARD. **b)** The
640 same plot after customisation to preference using a vector-based graphics package.
641 The data are in-situ long axis orientations of *Syntarsis rhodesiensis* (Dinosauria,
642 theropoda) bones from a sedimentary sequence in Zimbabwe (Roberts et al, unpubl.
643 data). n = 91, aperture = 17°, weighting factor = 0.95, equal area.
644
645 **Figure 6.** Finalising an output exported from the Octave version of MARD in a
646 vector-based graphics package. **a)** Original plot. **b)** Final plot following the
647 positioning of a circle within the initial square, the latter removed and modification to
648 preference. Dataset and applied parameters are the same as Fig. 5. n = 91, aperture =
649 17°, weighting factor = 0.95, equal area.
650
651 **Figure 7.** Unmodified output from the Excel version of MARD, prior to any
652 customisation. Dataset and applied parameters are the same as figs. 5 & 6. n = 91,
653 aperture = 17°, weighting factor = 0.95, equal area.
654
655
656 **Figure 8.** Microfracture orientations in garnet porphyroclasts within the Mtilikwe
657 shear zone, Zimbabwe (Blenkinsop & Kisters, 2005). n = 149, aperture = 9°,
658 weighting factor = 0.9, equal area.
659

Figure 9. Porphyroblast inclusion trail pitches in 2-dimensional section in andalusite and cordierite from the Cooma Complex of S.E. Australia shown on a single moving average plot. n (andalusite) = 1446. n (cordierite) = 1806. Measurements extracted from orientated vertical thin sections orthogonal to the strike of the internal foliation to ensure maximum pitch representation. The opacity of the cordierite has been reduced to 90% such that the andalusite plot may be observed underneath it simultaneously. Aperture = 9°, weighting factor = 0.9, equal area.

- MARD is an application for generating Moving Average Rose Diagrams
- Moving average rose diagrams are more informative than conventional binned equivalents
- MARD is available in three easy-to-use versions: MATLAB, GNU Octave, and Microsoft Excel
- MARD includes frequently used circular statistical measures

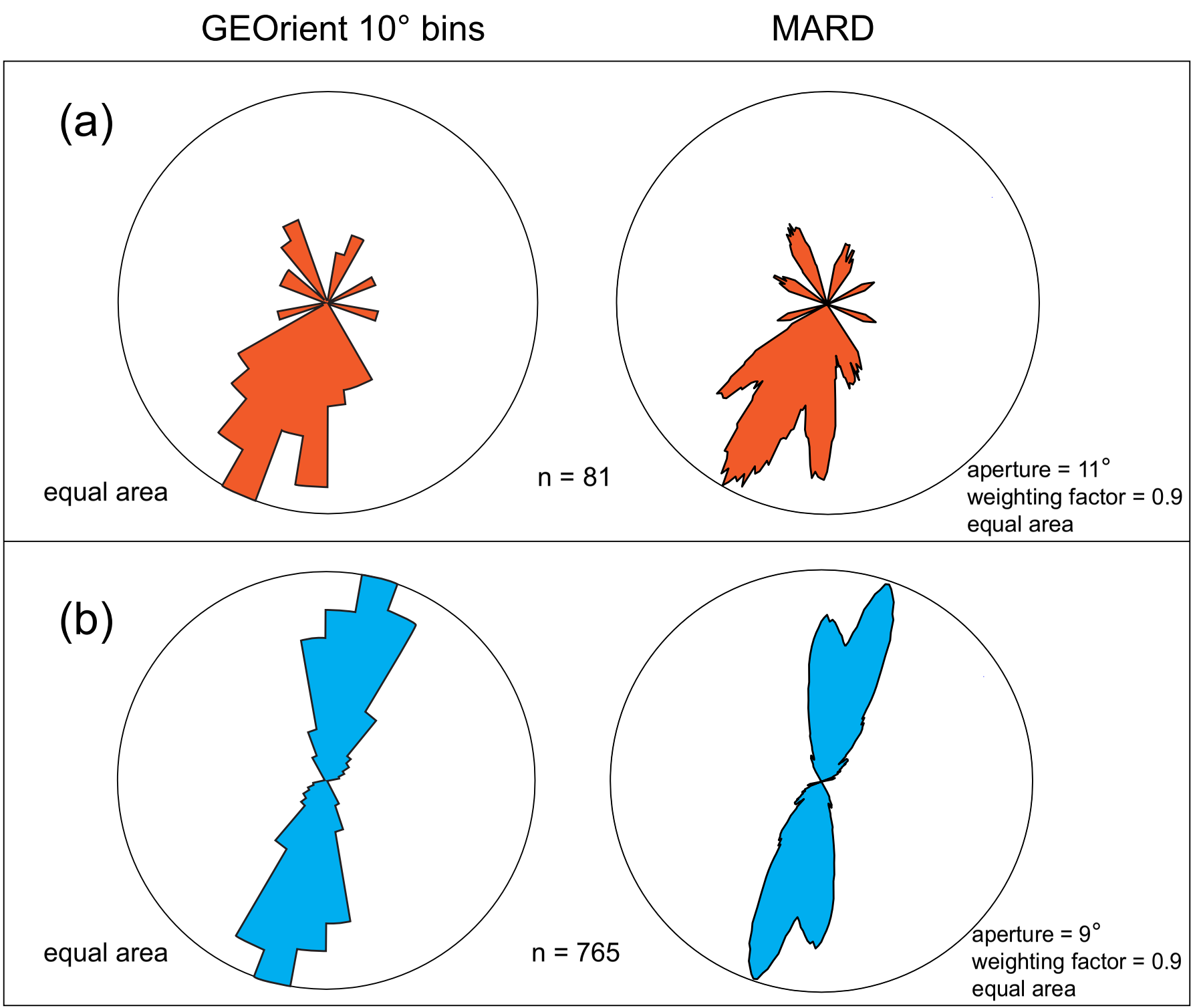

Figure(s)

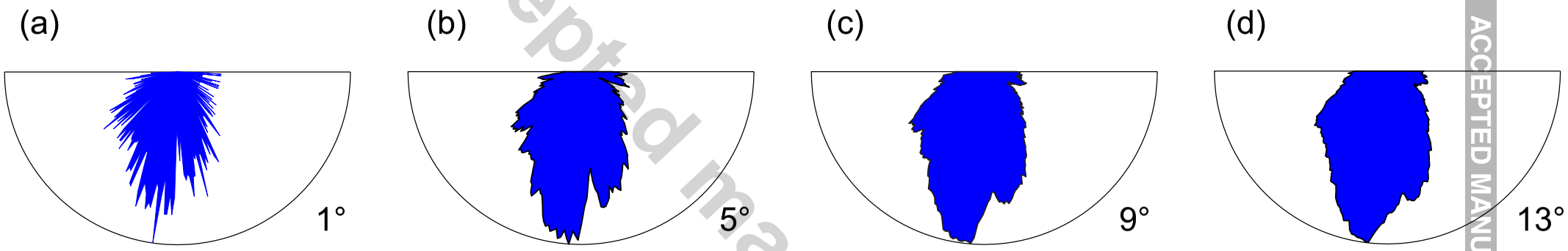

All plots: n = 1446, unweighted, equal area

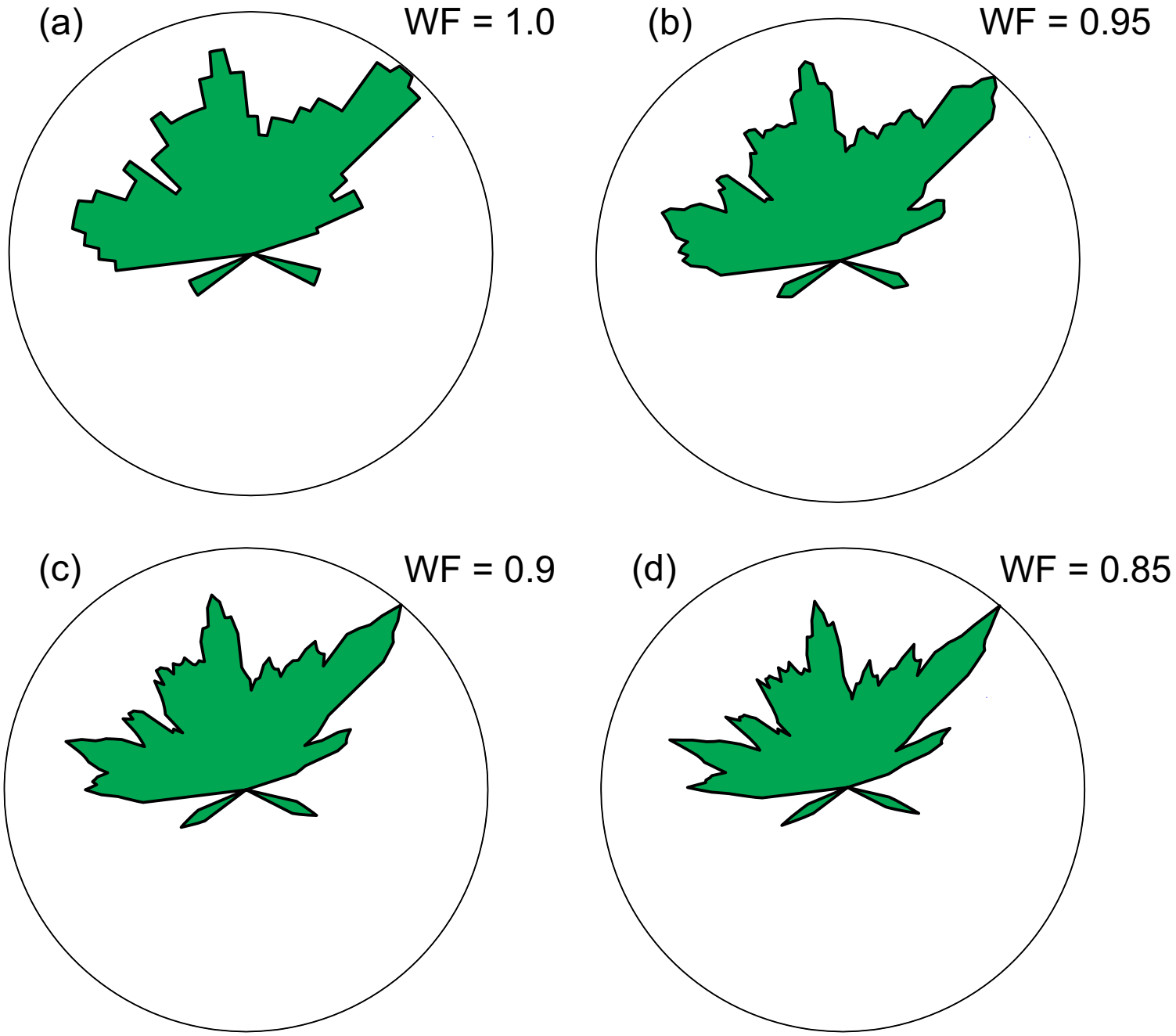

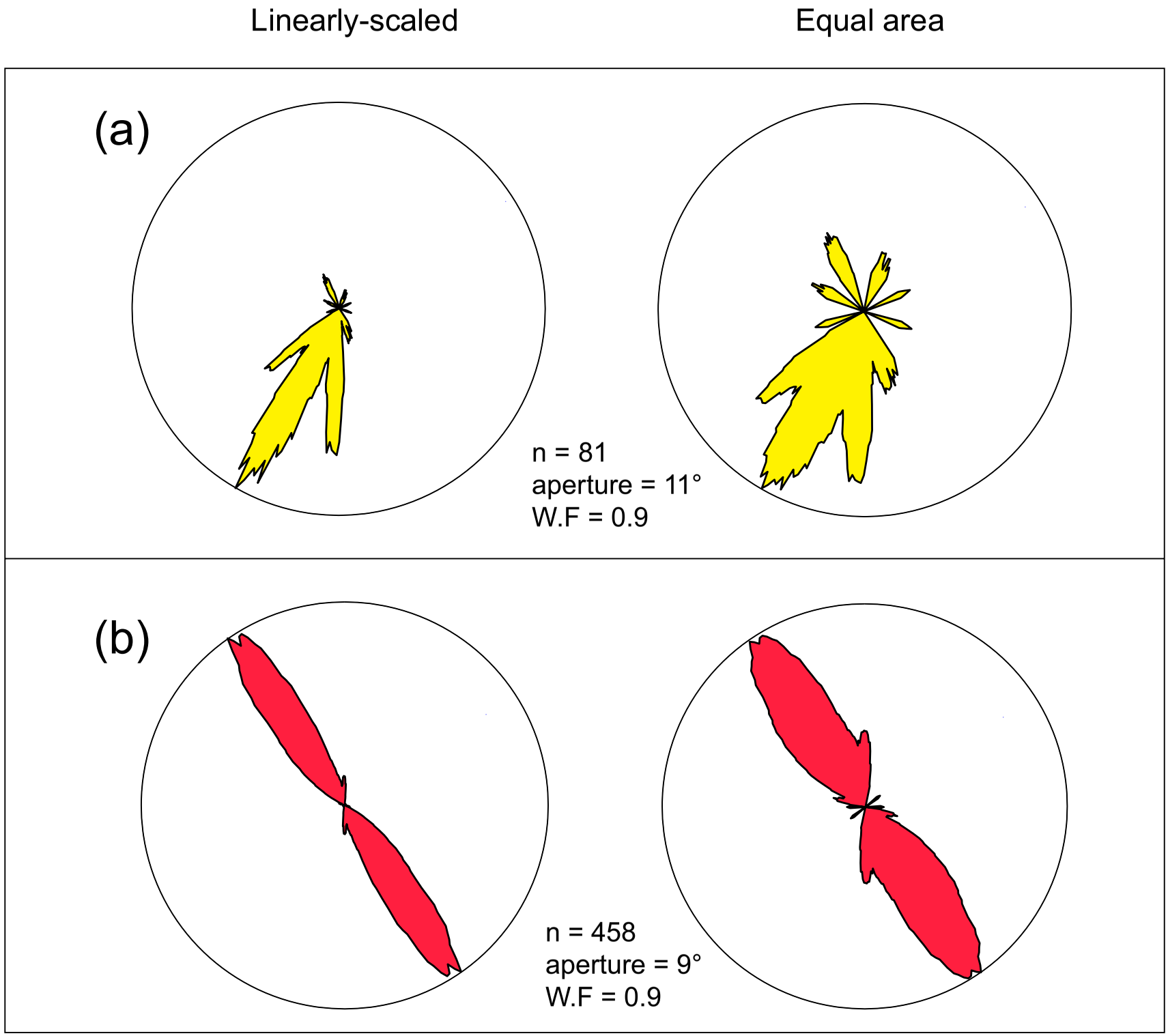

Figure(s)

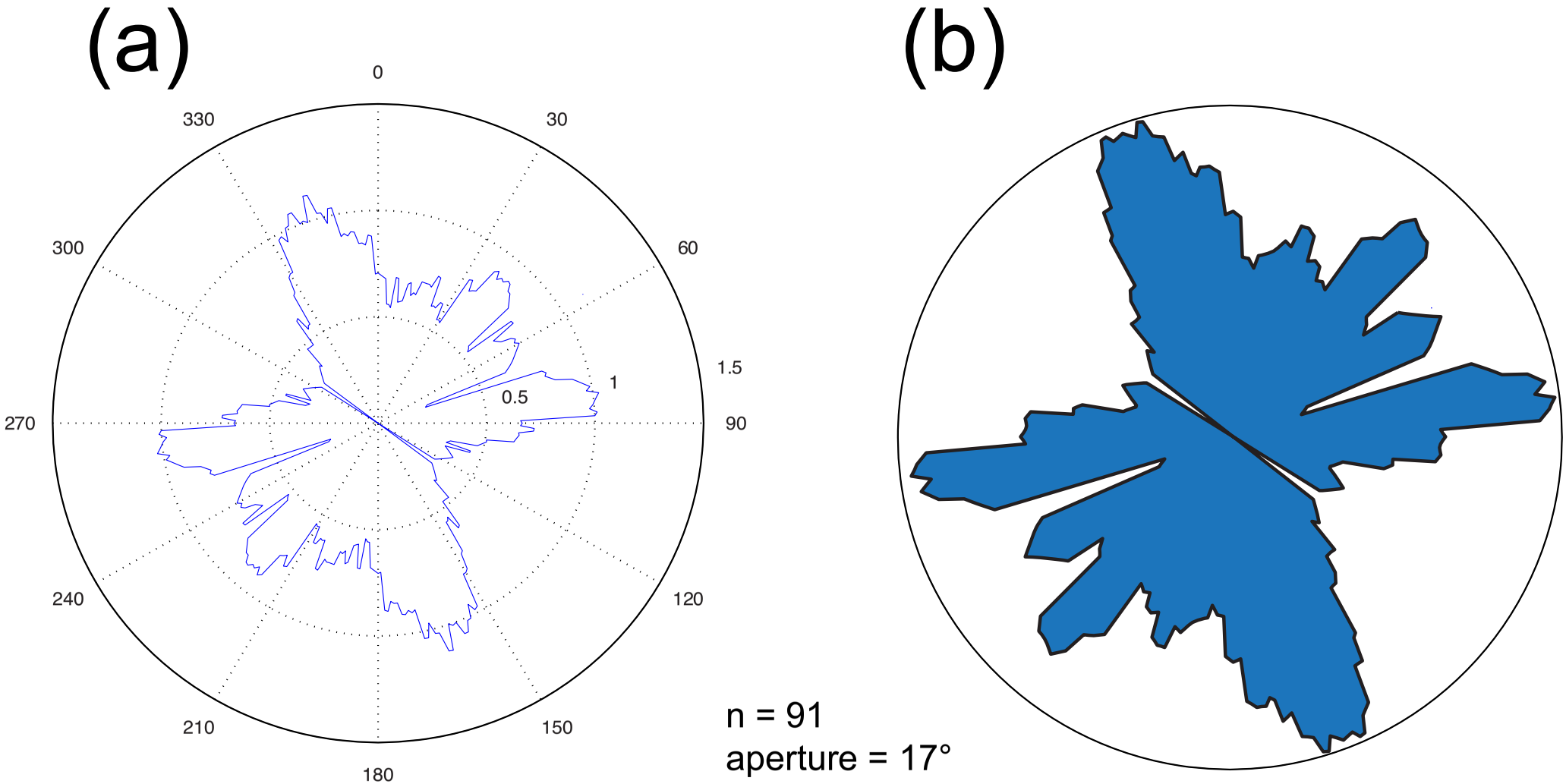
(a)
0
30
60
90
120
150
180
210
240
270
300
330
0.5
1
1.5
(b)
n = 91
aperture = 17°
W.F = 0.95
Equal area

Figure(s)

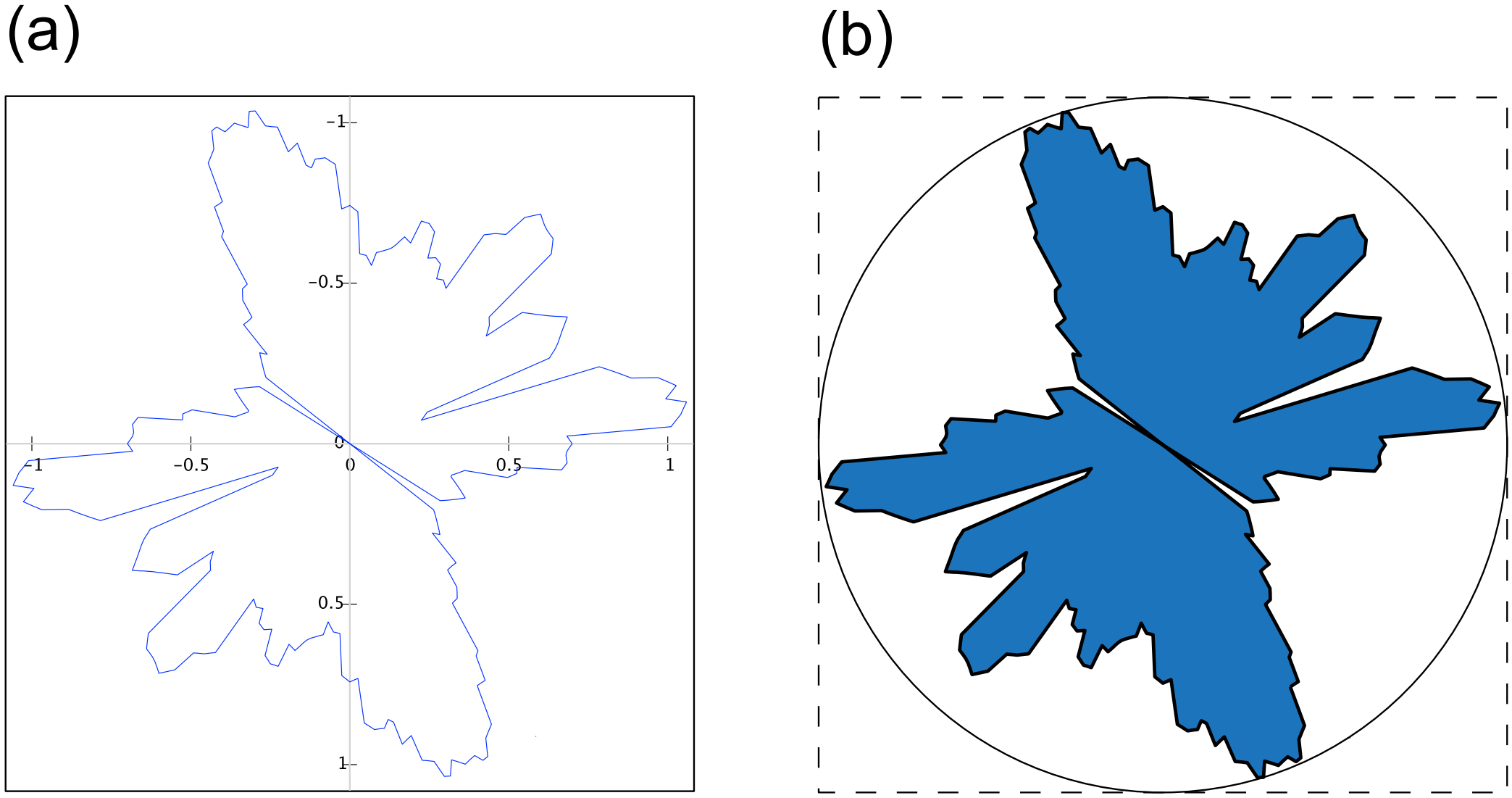

Figure(s)

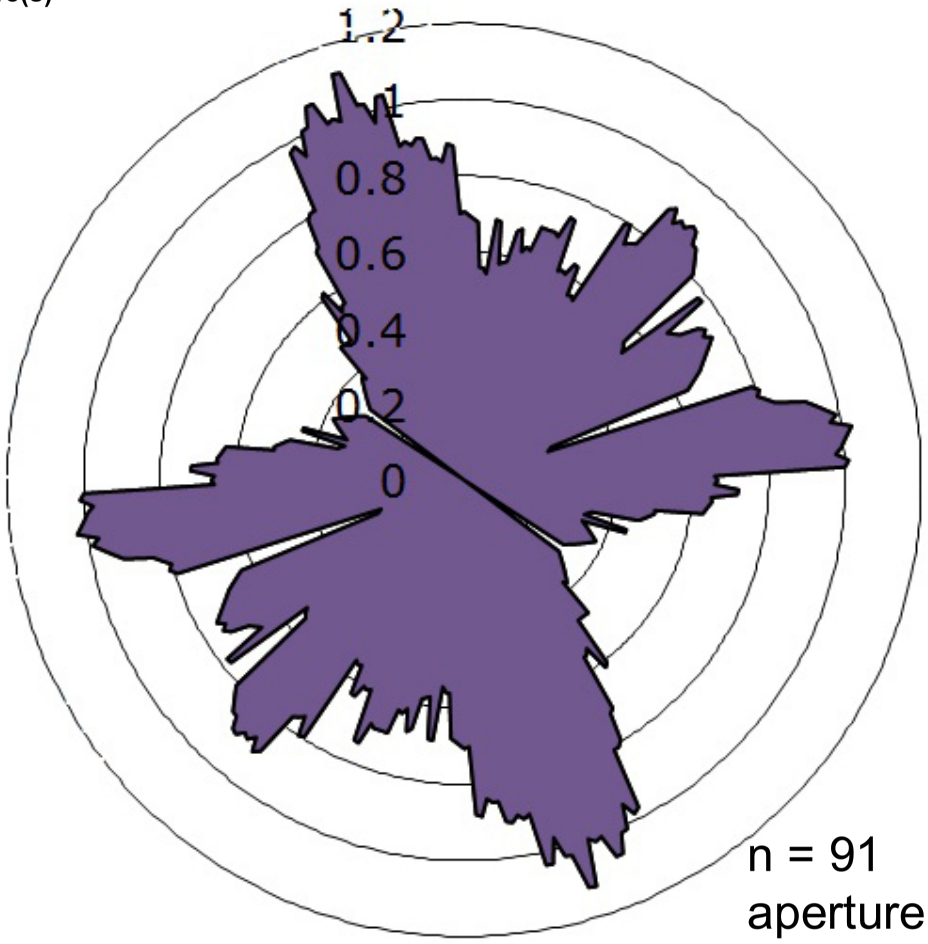

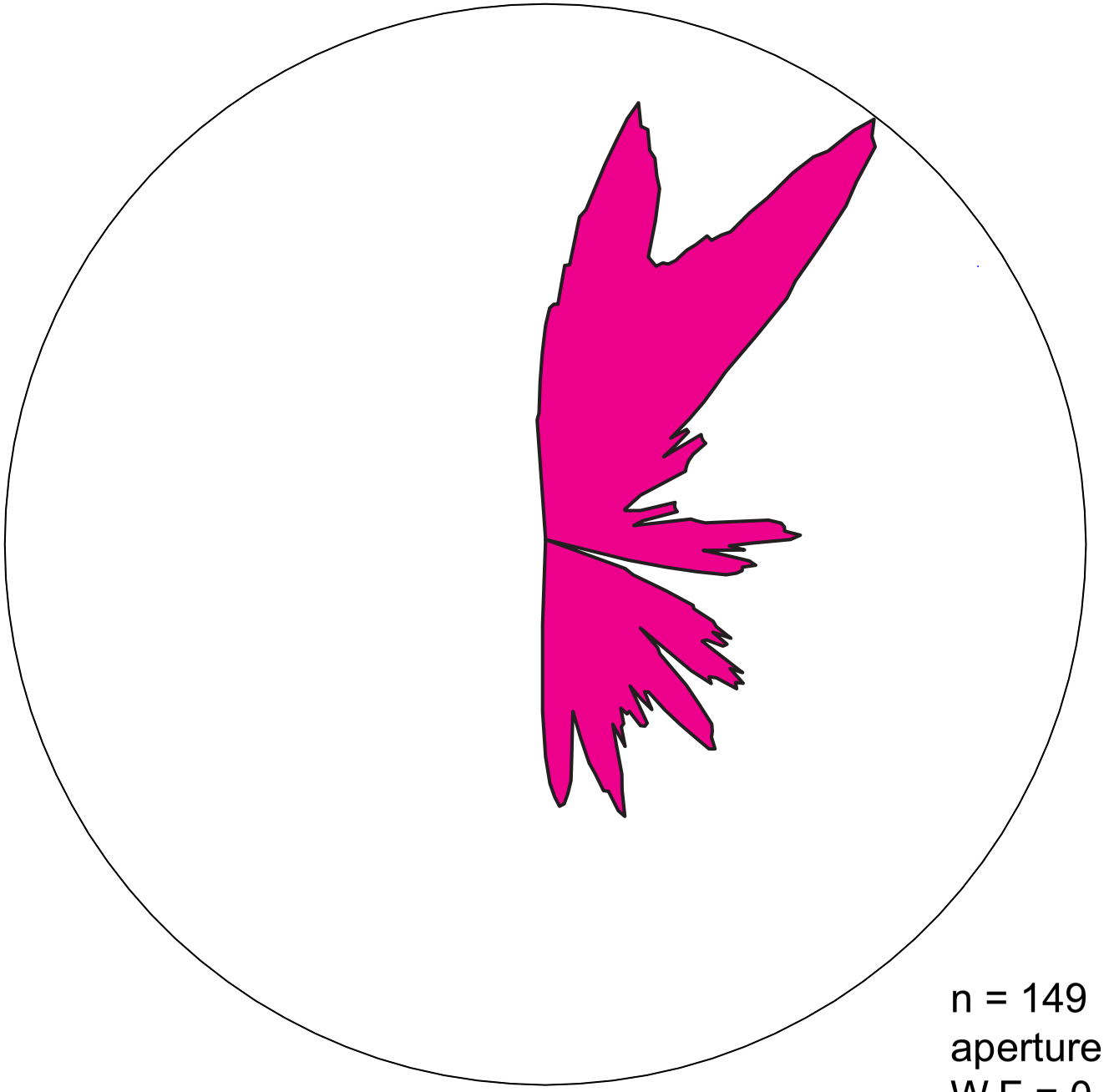

n = 149
aperture = 9°
W.F = 0.9
Equal area

Figure(s)

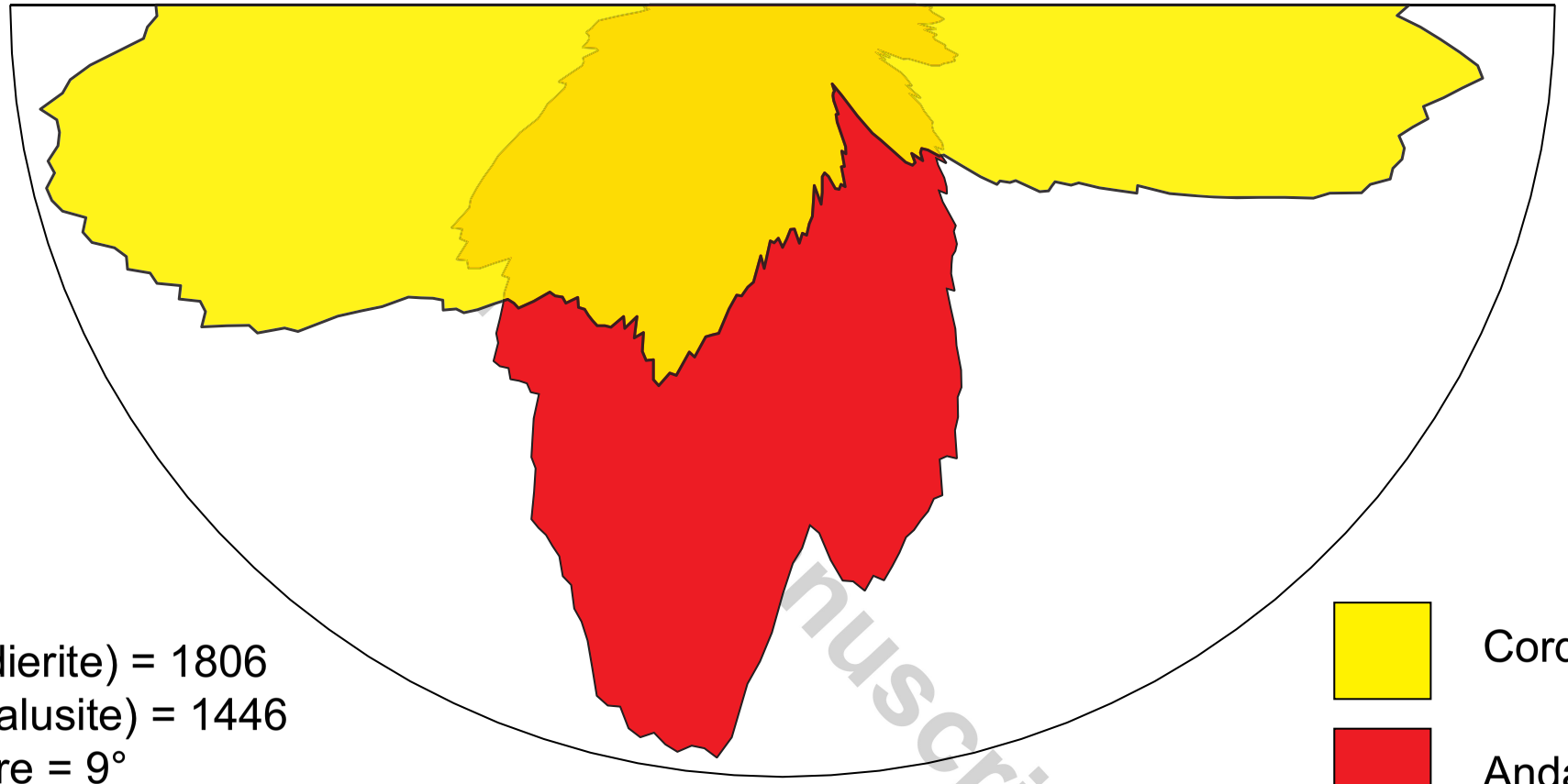

n (cordierite) = 1806
n (andalusite) = 1446
aperture = 9°
W.F. = 0.9
Equal Area

Cordierite
Andalusite
Both overlap

TABLE 1:

MATLAB®	Microsoft® Excel	GNU Octave
Requires a MATLAB® licence	Requires Microsoft Office (Note: not compatible with 2008 version for Macintosh).	Requires Octave + Graphics terminal (both freeware)
Command-line operated interface	Spreadsheet interface with drop-down menus	Command-line operated interface
Plots single or multiple datasets simultaneously	Single data set	Plots single or multiple datasets simultaneously
Data entry: compass azimuths or pitch inclinations	Data entry: raw azimuth data	Data entry: compass azimuths or pitch inclinations
Primary rose functions: uni-directional data, bi-directional data and lower semi-circle plot for pitches/dips	Uni-directional and bi-directional data functions only	Primary rose functions: uni-directional data, bi-directional data and lower semi-circle plot for pitches/dips
Plot formatting may be done 'in-house' via MATLAB® commands, or more comprehensively in a vector-based graphics package following exporting of the plot (recommended).	Plot formatting through Excel commands: some limitations	Formatting must be done in external vector-based graphics package (required).
Rose Diagram may be copied to clipboard, or saved as eps, ai, pdf, png, tif, jpg, or pcx.	Rose Diagram may be copied to clipboard, or saved as png, jpeg, pdf, gif or bitmap	eps format only
Circular Statistics: vector mean, mean resultant, circular standard deviation, circular variance/dispersion.	Circular Statistics: vector mean, mean resultant, circular standard deviation, circular variance/dispersion.	Circular Statistics: vector mean, mean resultant, circular standard deviation, circular variance/dispersion.

Code - MATLAB version of MARD

Code - GNU Octave version of MARD

Code - Excel macro version of MARD

Code - MARD ReadMe